

International Journal of Modern Physics B
© World Scientific Publishing Company

Numerical study on irreversible behavior of THz wave emission from intrinsic Josephson junctions

YOSHIHIKO NONOMURA

*Computational Materials Science Unit, National Institute for Materials Science,
Tsukuba 305-0047, Japan**

Received 13 September 2012

Recently novel current-driven resonant states characterized by the π -phase kinks were proposed in numerical and analytic studies on THz wave emission from intrinsic Josephson junctions based on the coupled sine-Gordon equation. In these states hysteresis behavior is observed with respect to the application process of current, and such behavior is due to nonlinearity in the Josephson coupling term. Varying strength of the critical current, there exists a critical strength for the hysteresis behavior in the fundamental mode, and at the critical strength the applied current at the emission peak coincides with the critical one, which means breakdown of superconductivity in actual systems. In higher-harmonic modes in the vicinity of the critical current, the strength of hysteresis becomes small and emission can be observed in the reverse process. Such “quasi-reversible” behavior may explain “reversible emission” reported in a recent experiment.

Keywords: THz wave emission; irreversibility; nonlinear effect.

1. Introduction

Recently the coupled sine-Gordon equation has been intensively studied as a model of THz wave emission from intrinsic Josephson junctions (IJJs).^{1,2} Novel emission states characterized by the π -phase kinks were proposed without external magnetic field.^{3,4} In these states hysteresis behavior is observed, namely strong emission in the current-increasing process with breakdown of the Ohm’s law and weak emission in the current-decreasing process. Such irreversible behavior is due to nonlinearity of the system, namely the Josephson coupling term.

In order to clarify the relation between the irreversible behavior and nonlinearity, an artificial parameter γ is introduced in the equation and strength of nonlinearity is varied continuously. In experiments, similar irreversibility has been widely reported. However, in a recent experiment⁵ reversible emission was reported in the larger-current region close to the critical current. This result also requires further study on the irreversible behavior. In Section 2, the model and formulation used in the present article are explained. In Section 3, dependence of irreversible behavior on

*nonomura.yoshihiko@nims.go.jp

the nonlinearity parameter γ is investigated in the fundamental mode. In Section 4, similar behavior is studied in higher-harmonic modes and relation with a recent experiment is discussed. The above descriptions are summarized in Section 5.

2. Model and formulation

Using material parameters of $\text{Bi}_2\text{Sr}_2\text{CaCu}_2\text{O}_8$ in Ref. 6, the inductive and capacitive couplings are given by $\zeta \approx 4.4 \times 10^5$ and $\alpha = 0.1$, respectively, and the latter can be neglected. Then, IJJs are described by the coupled sine-Gordon equation.⁷ When a nonlinear parameter γ ($= 1$ in the original equation) is further introduced, we have

$$\partial_{x'}^2 \psi_l = (1 - \zeta \Delta^{(2)}) (\partial_{t'}^2 \psi_l + \beta \partial_{t'} \psi_l + \gamma \sin \psi_l - J'), \quad (1)$$

with the layer index l and the operator $\Delta^{(2)}$ defined in $\Delta^{(2)} X_l \equiv X_{l+1} - 2X_l + X_{l-1}$. Quantities are scaled as $x' = x/\lambda_c$, $t' = \omega_p t$, $J' = J/J_c$; $\omega_p = c/(\sqrt{\epsilon_c} \lambda_c)$, with the penetration depth along the c axis λ_c , the plasma frequency in each layer ω_p , and the critical current J_c . Following Ref. 6, we take $\epsilon_c = 10$ and $\beta = 0.02$.

Neglecting temperature fluctuations and assuming homogeneity along the y axis, we have the two-dimensional formula (1). Following our previous study,⁸ we use the width of the junction $L_x = 86 \mu\text{m}$, the number of junctions $N = 4$, and the periodic boundary condition (PBC) along the c axis. Then, plasma velocity coincides with that of light in IJJs, and possible spatial inhomogeneity of ψ_l is taken into account.

We use a simplified version⁹ of the dynamical boundary condition,¹⁰ where effects outside of the sample are only included in the relation between dynamical parts of the rescaled electric and magnetic fields, $\tilde{E}'_l = \mp Z \tilde{B}'_l$, with the surface impedance $Z = 30$. Here E'_l and B'_l are related with ψ_l as $\partial_{t'} \psi_l = E'_l$ and $\partial_{x'} \psi_l = (1 - \zeta \Delta^{(2)}) B'_l$, respectively. The sample along the x axis is divided into 80 numerical grids for the fundamental mode and lower-harmonic modes, and into 160 numerical grids for higher-harmonic modes. Calculations are based on the RADAU5 ODE solver.¹¹

3. Hysteresis in the fundamental mode with varying nonlinearity

First, hysteresis behavior of the equation (1) in the fundamental mode ($n = 1$; n : number of node) is investigated for various values of γ . In the current-increasing (-decreasing) process, the system jumps from the upper (lower) edge to the next (previous) harmonic mode with the same current. Then, the strength of hysteresis can be visualized as the difference of currents between corresponding edges. Here we concentrate on the I - V curve around the $n = 1$ emission peak, where the applied current J (scaled by J_c) is plotted versus voltage per layer due to normal current.

In Fig. 1(a), parameter dependence of the $n = 1$ upper edge and the $n = 2$ lower edge of the I - V curve is visualized by various symbols for a wide range of parameters between $\gamma = 1.0$ and 0.1 . As γ decreases from the original value $\gamma = 1$, the strength of hysteresis becomes smaller and smaller. Hysteresis is observed up to $\gamma = 0.2$, while it becomes invisible at $\gamma = 0.1$. Then, more precise measurement is made between $\gamma = 0.17$ and 0.13 as shown in Fig. 1(b). Hysteresis behavior is

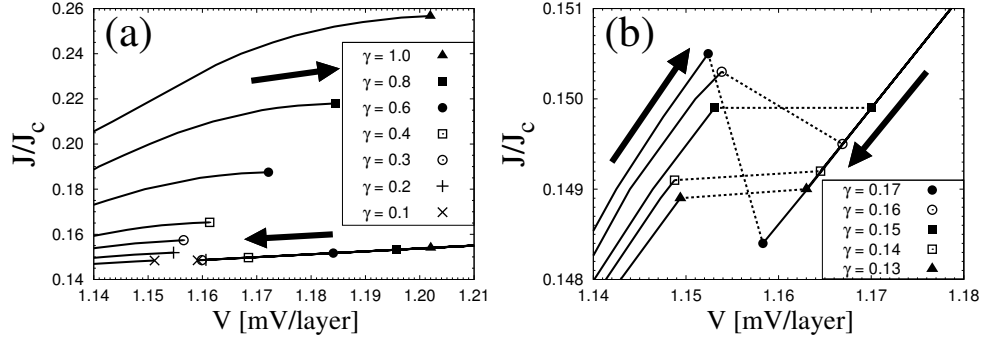


Fig. 1. I - V curve for various values of γ for (a) $\gamma = 1.0$ to 0.1 and (b) $\gamma = 0.17$ to 0.13 (expanded figure around the irreversible-reversible boundary). Edges of the $n = 1$ curve in the current-increasing process and the $n = 2$ curve in the current-decreasing process are visualized by various symbols. Corresponding edges are connected with each other with broken lines in the expanded figure in order to emphasize that hysteresis behavior vanishes for $\gamma \leq 0.15$.

observed up to $\gamma = 0.16$, and for $\gamma \leq 0.15$ current at the upper and lower edges becomes the same, or the current-varying process becomes reversible.

Fig. 1(b) reveals that $J/J_c = 0.150$ is satisfied at the emission peak for $\gamma = 0.15$, or $J = \gamma J_c$ holds at the irreversible-reversible boundary. Since γJ_c can be regarded as the scaled critical current in Eq. (1), this result means that the onset of reversible emission coincides with the breakdown point of superconductivity. That is, irreversible behavior might be equivalent to stability of superconductivity.

4. Irreversibility in higher-harmonic modes for $\gamma = 1$

In the previous section irreversible behavior in the fundamental mode is investigated by varying the critical current $J_c \rightarrow \gamma J_c$. Then, similar behavior can be expected in higher-harmonic modes for $\gamma = 1$ with larger current around the critical one J_c , which may be related with the experimental “reversible emission”.⁵

In Fig. 2(a), the I - V curve around the fifth harmonic ($n = 6$) and sixth harmonic ($n = 7$) modes is displayed. Although the current J exceeds J_c between these two modes, irreversible behavior is observed in the $n = 7$ mode (actually also in the $n = 8$ mode). Starting from Eq. (1), reversible behavior is not observed even for $J > J_c$ in higher-harmonic modes. Nevertheless, emission in higher-harmonic modes is different from that in the fundamental mode. As shown in Fig. 2(b), intensity of emission in the current-decreasing process (denoted by broken lines) is about half of that in the current-increasing process, and is expected to be observed in experiments. We consider such “quasi-reversible” behavior may explain “reversible emission” reported recently. Intensity of emission in the $n = 1$ mode is also shown in the inset, where intensity in the reverse process is about 10% of that in the forward process, or about one fourth of that in the reverse process for $n = 6$. Such weak emission may be invisible in experiments under impurity or rough surfaces.

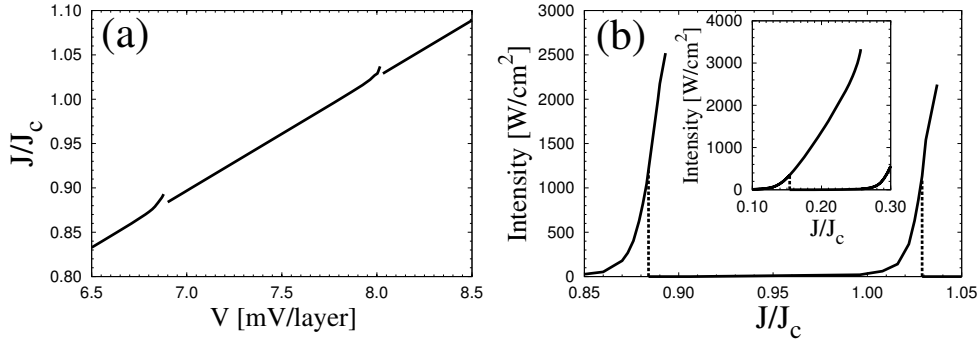


Fig. 2. (a) I - V curve and (b) current dependence of emission intensity in the $n = 6$ and $n = 7$ modes for $\gamma = 1$. Hysteresis is observed for both cases, and intensity in the reverse process is denoted by broken lines in (b), which is much larger than that in the $n = 1$ mode in the inset.

5. Summary

Novel resonant states in THz wave emission from intrinsic Josephson junctions are investigated numerically, and hysteresis is observed with respect to the application process of current. Such irreversible behavior is due to nonlinearity of the system, and we vary the strength of the Josephson coupling term. As long as the fundamental mode is observed, the maximum intensity of emission decreases monotonically as the nonlinearity parameter γ decreases, and hysteresis behavior vanishes when the applied current at the emission peak coincides with the scaled critical current γJ_c . That is, superconductivity and the irreversible behavior vanish at the same time.

Although hysteresis is still observed when the applied current exceeds the critical one in higher-harmonic modes, intensity of emission in the current-decreasing process is about half of that in the current-increasing process. Such “quasi-reversible” behavior in higher-harmonic modes is different from the irreversible one in the fundamental mode, which may explain “reversible emission” reported experimentally.

References

1. L. Ozyuzer *et al.*, *Science* **318**, 1291 (2007); see also K. Lee *et al.*, *Phys. Rev. B* **61**, 3616 (2000).
2. K. Kadowaki *et al.*, *Physica C* **468**, 634 (2008).
3. S. Lin and X. Hu, *Phys. Rev. Lett.* **100**, 247006 (2008).
4. A. E. Koshelev, *Phys. Rev. B* **78**, 174509 (2008).
5. H. Minami *et al.*, *Physica C* **470**, S822 (2010).
6. M. Tachiki *et al.*, *Phys. Rev. B* **71**, 134515 (2005).
7. T. Koyama and M. Tachiki, *Solid State Commun.* **96**, 367 (1995).
8. Y. Nonomura, *Phys. Rev. B* **80**, 140506(R) (2009).
9. S. Lin, X. Hu, and M. Tachiki, *Phys. Rev. B* **77**, 014507 (2008).
10. L. N. Bulaevskii and A. E. Koshelev, *Phys. Rev. Lett.* **97**, 267001 (2006), *J. Supercond. Nov. Mag.* **19**, 349 (2006).
11. <http://www.unige.ch/~hairer/software.html>